Radial Organization of Developing Preterm Human Cerebral Cortex Revealed by Non-invasive Water Diffusion Anisotropy MRI

Robert C. McKinstry[1], Amit Mathur[2,5], Jeffrey H. Miller[1], Alpay Ozcan[1], Abraham Z. Snyder[3], Georgia L. Schefft[2], C. Robert Almli[3,4], Shelly I. Shiran[7], Thomas E. Conturo[1] and Jeffrey J. Neil[1,5,6]

[1]Mallinckrodt Institute of Radiology, [2]Department of Neonatology, [3]Department of Neurology, [4]Program in Occupational Therapy, [5]Department of Pediatrics, [6]Division of Pediatric Neurology, St Louis Children's Hospital at the Washington University Medical Center, St Louis, MO, USA and [7]Department of Radiology, Rabin Medical Center, Sackler School of Medicine, Tel Aviv University, Tel Aviv, Israel

Cerebral cortical development involves a complex cascade of events which are difficult to visualize in intact, living subjects. In this study, we apply diffusion tensor imaging (DTI) to the evaluation of cortical development in human infants ranging from 26 to 41 weeks gestational age (GA). Apparent diffusion of water in cortex is maximally anisotropic at 26 weeks GA and anisotropy values approach zero by 36 weeks GA. During this period, the major eigenvector of the diffusion tensor in cerebral cortex is oriented radially across the cortical plate, in accord with a predominately radial deployment of its neuronal constituents. Values for the rotationally averaged water diffusion coefficient increase between 26 and 32 weeks GA, then decrease thereafter. These changes in DTI parameters are specific to cerebral cortex and reflect changes in underlying cortical architecture and formation of neuronal connections. Because of its correlation with tissue microstructure and non-invasive nature, DTI offers unique insight into cortical development in preterm human newborns and, potentially, detection of derangements of its basic cytoarchiteture.

Introduction

The remarkable events which comprise cerebral cortical development take place in a well-ordered manner. The majority of cortical neurons are generated near the cerebral ventricles and migrate towards the pial surface along a radially arranged scaffolding of glial cells, arriving at their final destination in the fetal cortical plate and assuming a well-defined, radially oriented, columnar organization (Rakic, 1972, 1988b). Subsequent cortical maturation involves elaboration of dendrites and axons, formation and regression of synaptic connections, and selective elimination of cell populations (Poliakov, 1959; Sidman and Rakic, 1982; Rakic, 1988a). To study the morphology and intricate biochemical processes involved in cortical development in animal model systems, *ex vivo* techniques such as electron microscopy, autoradiography, immunohistochemistry and analysis of spontaneous or induced mutations have been utilized (Cowan *et al.*, 1997; Rubenstein and Rakic, 1999). In contrast, studies of human regional brain differentiation have been done traditionally on *post mortem* tissue using classic histological methods (Poliakov, 1959; Sidman and Rakic, 1973, 1982; Honig *et al.*, 1996; Volpe, 2001) and only more recently with magnetic resonance imaging (MRI) of fixed tissue (Kostovic *et al.*, 2002) and *in vitro* analysis of living slice preparations (Letinic and Rakic, 2001, 2002).

In the present study, we evaluate cortical development in live human infants using a form of magnetic resonance imaging – diffusion tensor imaging (DTI). DTI is a means of measuring the translational motion of water within tissue and is sensitive to molecular displacements on the order of 10 μm. This motion is often referred to as the 'apparent diffusion' of water in acknowledgment of the fact that water motion in tissue may reflect processes in addition to stochastic, thermally driven Brownian motion (Neil, 1997).

One unique feature of DTI is that the directionality of water motion can be determined. A sample of pure water, for example, has water displacements which are equal in all directions (isotropic diffusion). In tissue, on the other hand, water motion is hindered by cellular constituents. If this hindrance is greater in one direction than another, water motion is anisotropic. For example, water molecules in white matter move less freely perpendicular to fibers than parallel to them because motion perpendicular to fibers requires passing through or around layers of myelin membrane, whereas motion parallel to them does not. Thus, water apparent diffusion in mature white matter is highly anisotropic. In this manner, DTI characterizes tissue microstructure. Three quantities extracted from DTI are particularly useful for microstructural characterization: the directionally averaged water apparent diffusion coefficient (D_{av}); the degree of anisotropy of water motion (A_σ); and the orientation along which water apparent diffusion is greatest (the direction of the major eigenvector of the diffusion tensor). D_{av} represents how freely water diffuses through tissue. D_{av} is greater when tissue water content is higher or when barriers to water motion, such as cell membranes, are widely spaced. For reference, D_{av} for pure water at body temperature is on the order of 3.0×10^{-3} mm^2/s, that for infant brain ranges from 1.0 to 2.0×10^{-3} mm^2/s (Huppi *et al.*, 1998; Neil *et al.*, 1998) and that for adult brain is on the order of 0.8×10^{-3} mm^2/s (Pierpaoli *et al.*, 1996; Shimony *et al.*, 1999). A_σ ranges from near zero for adult cerebral cortex (isotropic diffusion) to 0.5 for adult commissural white matter (Shimony *et al.*, 1999). The orientation of the major eigenvector of the diffusion tensor, since it is parallel to the predominant fiber direction in white matter, has been used to trace the course of white matter tracts in intact brain (Conturo *et al.*, 1999; Mori *et al.*, 1999; Basser *et al.*, 2000).

Using current DTI methodology, water diffusion in the adult cerebral cortex is isotropic or very mildly anisotropic (Shimony *et al.*, 1999; Sorensen *et al.*, 1999). However, a previous study from our laboratory indicated that cerebral cortex in premature infants may be strongly anisotropic transiently during development [see fig. 2 of Neil *et al.* (Neil *et al.*, 1998)]. Similar observations have been made in studies of live cat (Baratti *et al.*, 1997) and piglet (Thornton *et al.*, 1997), as well as fixed mouse brain (Mori *et al.*, 2001). In this study, we characterize water diffusion in cortical gray matter in a series of human neonates at gestational ages (GA) ranging from 26 to 41 weeks. The orderly progression of water diffusion parameters during development, as it reflects changes in cortical microstructure, may ultimately provide novel information regarding both cortical development and abnormalities of that development.

Materials and Methods

Subjects

All studies were approved by the Washington University Human Studies Committee. Infants were studied only after parental consent was obtained. The study included an initial scan within the first 36 h after birth. A total of 24 infants were imaged. Ten of these underwent a single scan within the first 2 days of life as part of a previous study (Neil *et al.*, 1998). The remaining 14 underwent two scans, one near the time of birth and a second prior to discharge from the hospital.

Preterm infants were recruited from the neonatal intensive care unit and special care nursery. Infants were all products of uncomplicated deliveries. Their GAs ranged from 26 to 41 weeks. The GA was based on the mother's last menstrual period, the infant's Ballard score (Ballard *et al.*, 1991) and fetal ultrasound (if available). Subjects were excluded if these GA estimates did not agree to within 1 week. The GAs used for data analysis were the averages of these values. Infants were also excluded if there was evidence of drug exposure *in utero*, brain injury (seizures, altered mental status), significant hypoxia (reduced urine output, cardiac injury requiring administration of pressor agents), severe respiratory distress, or congenital malformations. In addition, infants on continuous positive airway pressure were excluded because of equipment incompatibility with the MR scanner. Infants whose MR scan prior to discharge from the hospital were included in the data were those for whom there were no known complications during the hospital course that would cause cortical injury.

Infants were transported in an incubator to and from the MR scanner under supervision of a pediatric transport nurse and a physician. Infants were swaddled in warm sheets/blankets, placed on the scanner table on an MR-compatible chemical heating pad (Portawarm mattress; Abbott Laboratories, Abbott Park, IL) and their heads restrained with soft cushions. No sedation was used. The infant's heart rate and oxygenation were monitored via pulse-oximetry. Infants needing ventilator support were hand ventilated for the duration of the study.

The data were obtained on a 1.5 T Siemens Magnetom Vision system (Erlangen, Germany) using a circularly polarized extremity coil. Conventional T_1- and T_2-weighted MR scans were obtained using contiguous, 5 mm, transverse sections. The field of view (FOV) was 150 mm, yielding 0.6 × 0.6 mm in-plane resolution. DTI consisted of single-shot, multisection, spin echo planar imaging (EPI) with FOV 240 mm, in-plane resolution 1.9 × 1.9 mm interpolated to a 256 × 256 matrix for display and analysis, repetition time (T_R) 3000 ms and echo time (T_E) 106 ms. Four tetrahedrally oriented, diffusion-weighted images (diffusion sensitivity, b = 800 s/mm^2), three orthogonally oriented, diffusion-weighted images (b = 340 s/mm^2) and a reference T_2-weighted intensity image (b = 0 s/mm^2) were obtained at each transverse section. Two, nine-slice DTI acquisitions were obtained and manually interleaved. Each individual DTI acquisition with image transfer took ~2 min. Wherever possible, each slice location was repeated three times to provide data redundancy for reconstruction of images should the infant move during the scan. The typical total time in the scanner was 40 min for conventional and DTI data collection.

Image Analysis

All raw diffusion DTI MR images were realigned in two dimensions using a combination of intra- and cross-modality affine realignment procedures to correct for image displacements and linear stretch or shear due to eddy currents (Neil *et al.*, 1998). For each pixel, the elements of the diffusion tensor were derived from this combination of reference T_2-weighted images, tetrahedral diffusion measurements and perpendicular diffusion measurements (Neil *et al.*, 1998; Shimony *et al.*, 1999). Image quality was assessed by evaluating anisotropy maps. These maps are extremely sensitive to changes in image quality caused by movement artifact or poor signal-to-noise ratio. If anisotropy values were excessively high for the region of the centrum semiovale, a region of typically low anisotropy, the data set was not used.

A single contiguous region-of-interest (ROI) encompassing the parietal and occipital cortex was outlined on T_2-weighted MR images, where there is especially strong contrast between the developing gray and white matter in the premature brain. These ROIs were translated to DTI maps and sampled for water apparent diffusion coefficient and anisotropy using ANALYZE software (Mayo Foundation Rochester, MN). In an effort to minimize within-slice partial volume effects, which may contribute to inaccurate measurement of DTI indices, cortical regions were outlined on the slice of interest and then verified to include only the cortex on the image slices above and below the slice of interest. To accomplish this, the outline of parietal and occipital cortex from the slice of interest was projected onto the slices above and below the slice of interest. Any region that was not composed of gray matter on these slices was removed from the outline (such regions typically contained cerebrospinal fluid due to curvature of the cortex). ROIs from occipital and parietal cortex were chosen for analysis to avoid magnetic susceptibility artifacts that sometimes arise in frontal and temporal cortex due to the proximity of nasal cavities or auditory canals. All ROI placements were verified by a CAQ-certified neuroradiologist (R.C.M.) and a board certified pediatric neurologist (J.J.N.). 'Whisker plots' were generated using Matlab (MathWorks Inc., Natick, MA) to superimpose lines representing the projection of the major eigenvector onto the D_{av} map.

Data were analyzed using a Spearman rank correlation. The relationship between GA and D_{av} for cortex was analyzed using the general linear model procedure (SAS Software, Cary, NC).

Results

A total of 24 infants were evaluated for the study. Of these, 14 underwent two scans, giving a total of 38 available studies. Of these 38 studies, 28 were sufficiently free of movement artifact for further analysis. The infants selected for study were those with relatively uneventful prenatal and perinatal courses. Nevertheless, the majority were born prematurely and premature birth is often associated with other complications. Pregnancy was complicated by gestational diabetes mellitus for one, pregnancy-induced hypertension for two, twin gestation for four and proteinuria for two. Prolonged rupture of membranes was present for three, though none of these three infants had sepsis detected on routine blood, cerebrospinal fluid and urine culture. None of these complications would be expected to lead directly to brain injury. Of the 24 infants studied, six were delivered by Caesarean section and the rest vaginally. All infants were healthy at delivery except for those needing ventilator support due to lung immaturity.

Figure 1 shows axial images from the level of the basal ganglia at differing GAs. As seen on the T_1-weighted images, the gyral pattern of the cortex becomes more complex between 26 and 35 weeks GA. On the D_{av} maps, cerebral cortex appears dark because D_{av} values in cortex are lower than those of white matter at this age (Huppi *et al.*, 1998; Neil *et al.*, 1998). In the corresponding A_σ maps, the cerebral cortex shows relatively high anisotropy at 26 and 31 weeks GA, but this diminished by 35 weeks GA. Note that cortical anisotropy is not seen consistently in the frontal region (see Discussion). Note also that the outermost rim of high anisotropy present in the images is an artifact. In regions where signal is low (such as in the skull), anisotropy values are artifactually increased because the DTI acquisition parameters are not optimized for the signal from this particular area – instead, they are optimized for signal from brain. The anisotropy maps have been cropped so that the areas outside the skull are not shown. Relatively high anisotropy is also present in central, projectional and commissural white matter tracts, including the genu and splenium of the corpus callosum as well as the internal and external capsules.

Figure 2 shows the values for A_σ as a function of GA. For the posterior limb of the internal capsule (Fig. 2*A*, closed circles), these values gradually increase with increasing GA (rank sum = 0.97, $P < 0.01$, Spearman rank correlation). Values for the head of the caudate nucleus (Fig. 2*A*, open circles), on the other hand, are consistent with zero and remain so throughout the GAs studied (rank sum = –0.11, $P > 0.10$). (Note that A_σ values are

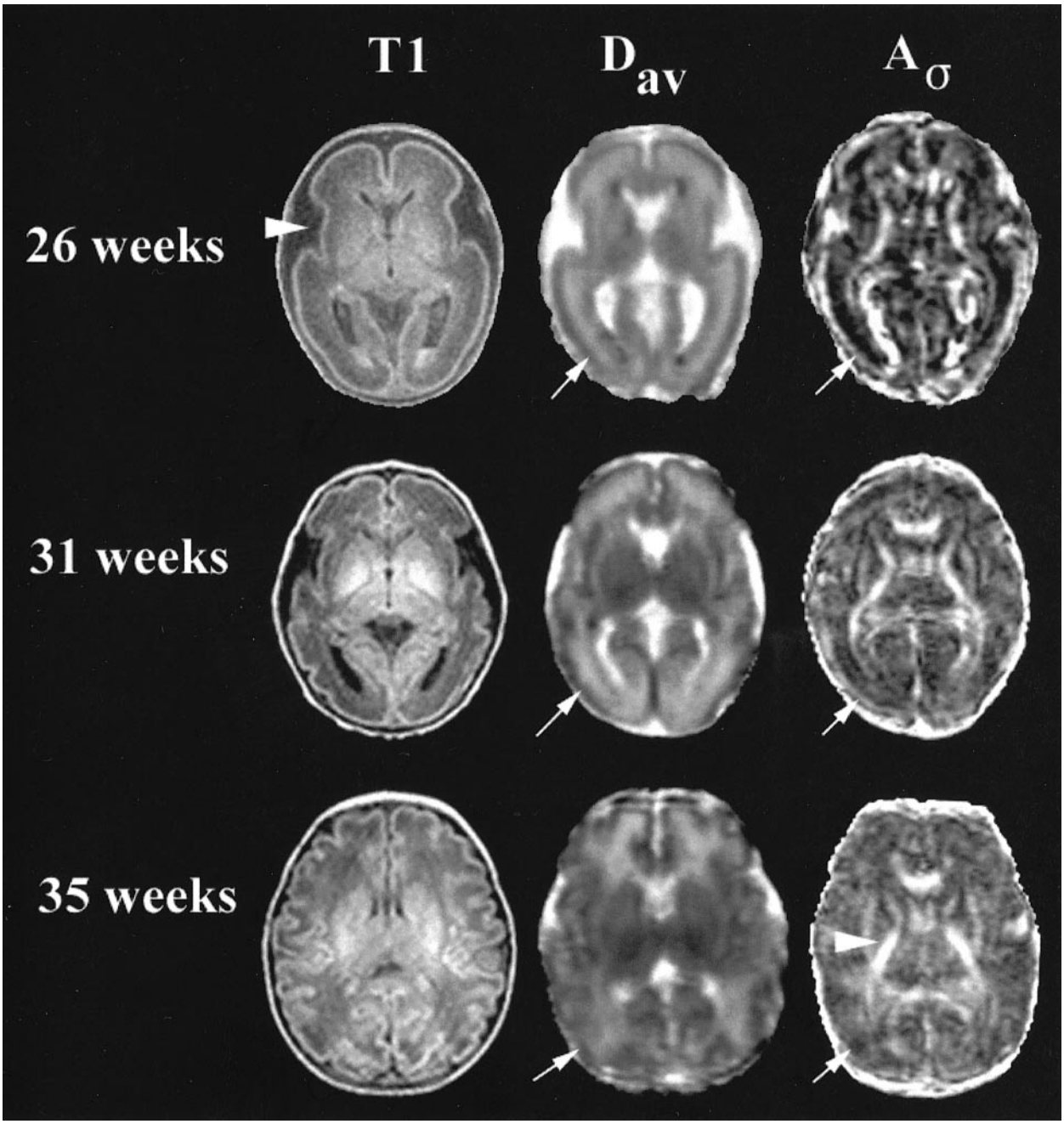

Figure 1. Axial images obtained at the level of the basal ganglia from infants studied at 26, 31 and 35 weeks GA. Anterior is up and posterior is down. From left to right, the columns show T_1-weighted images, D_{av} maps and A_σ maps. Note the cortical development, particularly opercularization of insular cortex (arrowhead on T_1-weighted image from 26 weeks GA) and sulcation, that takes place between 26 and 35 weeks GA. Cortical gray matter (arrows) has lower values for D_{av} than white matter in premature infants, though this difference diminishes with increasing GA. Anisotropy values are high (i.e. bright on anisotropy maps) for cerebral cortex at 26 and 31 weeks, but not at 35 weeks, GA (arrows). In contrast, anisotropy values increase for the internal and external capsules with increasing GA. The arrowhead on the A_σ map from 35 weeks GA points to the posterior limb of the internal capsule.

calculated as the standard deviation of the magnitudes of the principal eigenvalues. These magnitudes are never exactly equal, even for isotropic diffusion, because of noise in the measurement. As a result, As values do not reach zero, but approach a 'noise floor.' For this study, the noise floor is ~0.05.) For cerebral cortex (Fig. 2*B*), there is a statistically significant decline in diffusion anisotropy with increasing GA (rank sum = –0.94, $P < 0.01$).

Values for D_{av} as a function of GA are shown in Figure 3. D_{av} values for the posterior limb of the internal capsule (Fig. 3*A*, closed circles) and head of the caudate (Fig. 3*A*, open circles) decrease monotonically with increasing GA. Spearman rank correlation of data from the posterior limb of the internal capsule show rank sum = –0.92, $P < 0.01$; for the head of the caudate, rank sum = –0.66, $P < 0.01$. Values for cortex (Fig. 3*B*), on the other hand, increase between 26 and 32 weeks GA and decrease thereafter. These data were examined using a polynomial regression approach to identify the degree of polynomial required to fit the data appropriately. Using a model involving linear, quadratic and cubic terms, the cubic term was not

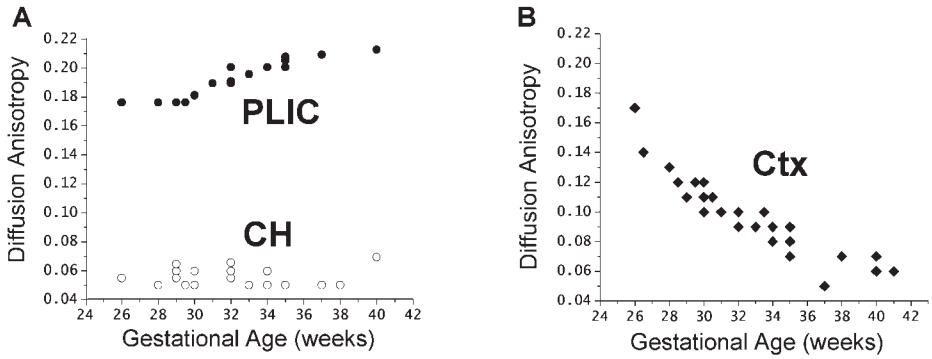

Figure 2. Plots of diffusion anisotropy versus GA. In panel (*A*), values from the posterior limb of the internal capsule [PLIC, a region destined to be myelinated by term (Brody *et al.*, 1987), filled circles] and the caudate head (CH, a gray matter area containing a minimum of white matter fibers, open circles) are shown for reference. Note that the values for the caudate head are consistent with zero because of the 'noise floor' present in anisotropy measurements. Panel (*B*), for which the axes are the same as those of panel (*A*), shows data from parietal and occipital cortex (Ctx). Note that values for anisotropy reach the noise floor by 36 weeks GA.

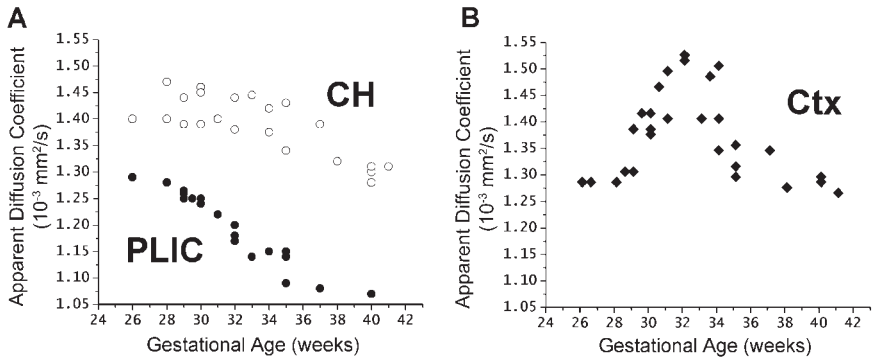

Figure 3. Plots of D_{av} versus GA. In panel (*A*), values from the posterior limb of the internal capsule (PLIC, filled circles) and the caudate head (CH, open circles) are shown for reference. D_{av} values for the posterior limb of the internal capsule and caudate head decrease monotonically with increasing GA. Values from cortex (Ctx) are shown in panel (*B*) using the same axes as panel (*A*). D_{av} values for cortex increase between 26 and 32 weeks GA, then decrease.

statistically significant ($P > 0.05$). After dropping this term and using a model involving linear and quadratic terms, R^2 was 0.48 and the quadratic term was statistically significant ($P < 0.01$). Finally, using a model with only a linear term, R^2 fell to 0.04. Thus, fitting the data to a quadratic expression is statistically justifiable and reflects the observation that D_{av} values vary with GA in a nonlinear fashion (Fig. 3*B*).

The orientation of the major eigenvectors of the diffusion tensors is shown in Figure 4. For cerebral cortex, the orientation is primarily radial (orthogonal to the cortical surface) at 26 weeks GA (Fig. 4*A*). By 35 weeks GA, this orientation is no longer detectable (Fig. 4*B*) as the diffusion anisotropy values approach the noise floor (Fig. 2*B*). For central white matter, the orientation of the major eigenvectors follows the general direction of white matter tracts in the genu and splenium of the corpus callosum (Fig. 4*A*,*B*).

Discussion

The key finding of this study is that the cerebral cortex demonstrates a pronounced radial organization that is clearly visible at 26 weeks GA, but disappears by 36 weeks GA. One means of visualizing this mathematical result is by representing water diffusion with a diffusion ellipsoid, a construct which has been used for decades to describe diffusion in three dimensions. If one places a drop of colored dye into a glass of water and allows it to diffuse for some time, the shape assumed by the dye is a sphere because dye molecules are equally likely to diffuse in any direction (provided they do not encounter the walls of the container). If a dye droplet is placed into the white matter of brain and allowed to diffuse for some time, the resultant shape is not spherical. Rather, it is similar to a rugby ball with the long axis oriented parallel to the white matter tracts. This non-spherical shape is present because the dye molecules move more freely parallel to axons than orthogonal to them, as motion orthogonal to fibers is more strongly restricted by barriers to diffusion, such as myelin layers. A_σ is a means of quantifying this phenomenon. When diffusion is isotropic ($A_\sigma = 0$), the ellipsoid shape is spherical; when diffusion is anisotropic ($A_\sigma > 0$), the ellipsoid shape is more akin to the shape of a rugby ball. The longer and thinner the ellipsoid, the higher the value for A_σ. Such prolate ellipsoids are shown schematically in Figure 5.

Water diffusion properties are strongly influenced by tissue microstructure. It is generally agreed that diffusion anisotropy in white matter is due to the ordered architecture of axons and myelin in fiber bundles (Beaulieu and Allen, 1994). However, some other microstructural explanation is called for in developing cerebral cortex, as ordered bundles of axons are absent. Although adult cerebral cortex is believed to operate as an ensemble of functionally linked radial columns (Mountcastle, 1997), this organization is obscured in adult cerebrum by the predominance of laminar organization. Here, we report that this basic, radial organization is clearly visible during a specific developmental time period. Neuronal migration from the ventricular zone to the cortical plate in the human fetal cerebrum is essentially complete by 26 weeks GA (Sidman and Rakic, 1973; Kostovic *et al.*, 2002). Therefore, the microstructural changes

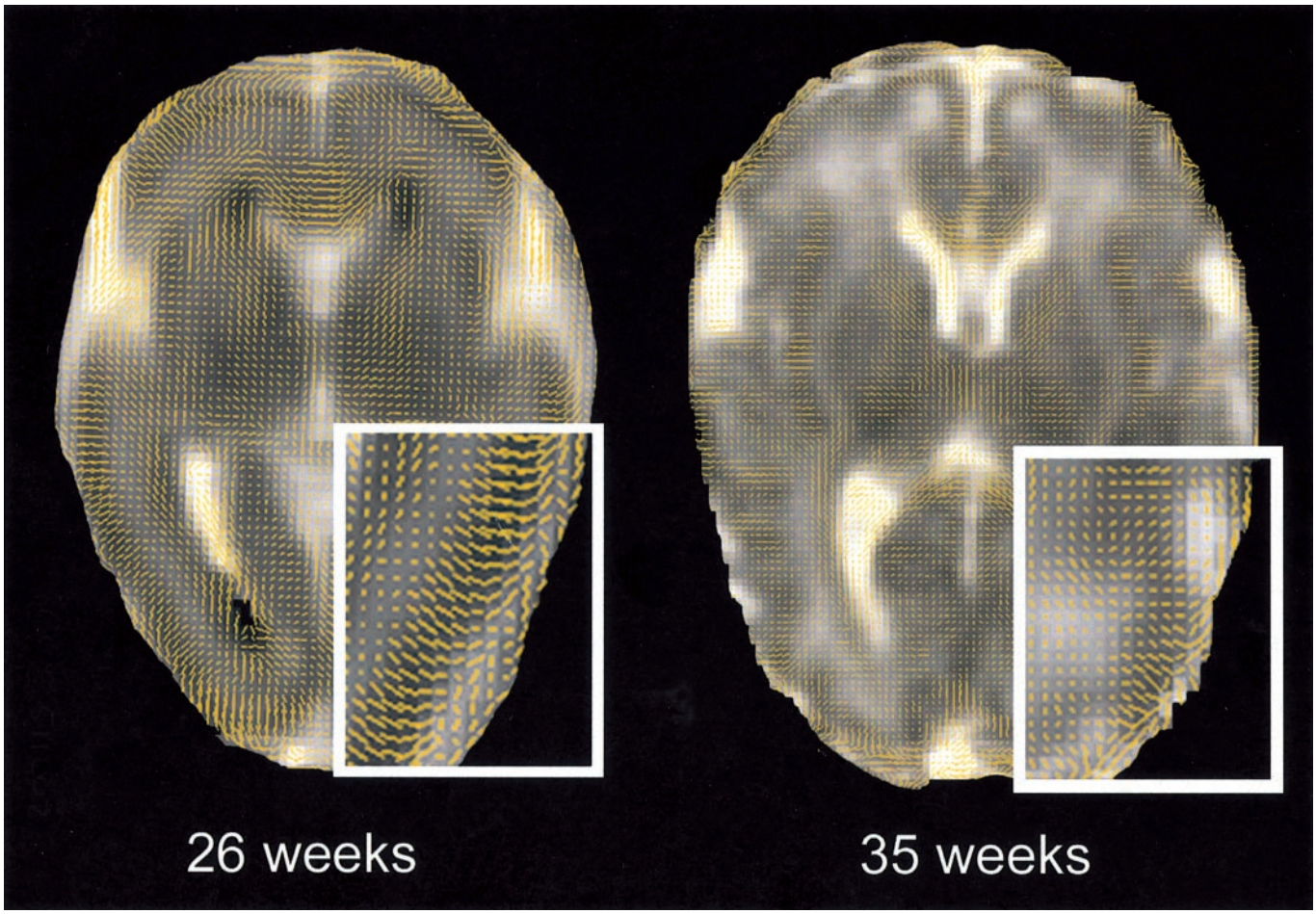

Figure 4. Diffusion whisker plots overlaid on D_{av} images from infants of 26 and 35 weeks GA. The line segments are the projection of the major eigenvector onto the plane of the image and represent the orientation of the major eigenvectors. The insets with white borders are magnifications of the parieto-occipital regions of the images. Note that the major axes are oriented radially in cortex at 26 weeks GA. By 35 weeks GA, this feature is much less evident. In both images, organization of whiter matter is visible in the genu of the corpus callosum. The dark areas at the occipital horn of the lateral ventricles of the image from 26 weeks GA is due to small intraventricular hemorrhages layering dependently.

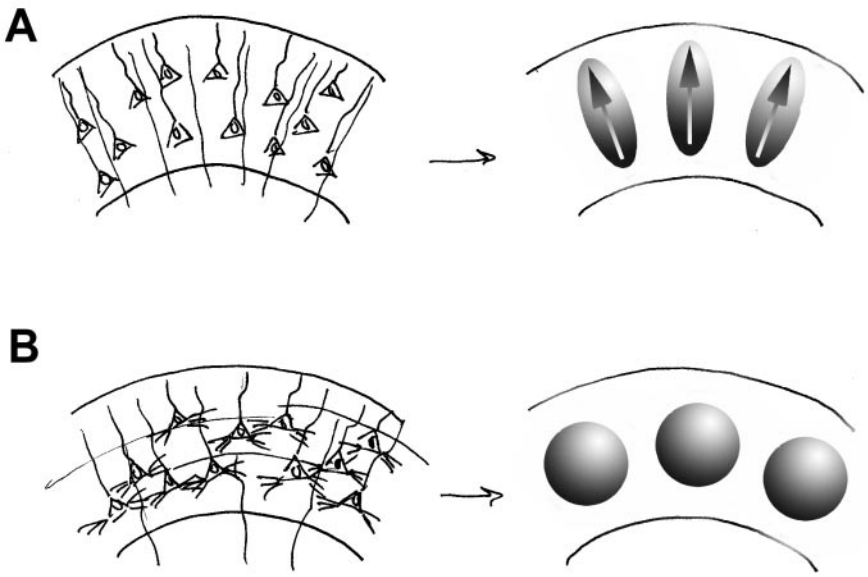

Figure 5. A diagram depicting our proposed explanation for cortical anisotropy. On the left are representations of cortical structure. On the right are the corresponding diffusion ellipsoids. At 26 weeks GA (*A*), radial glial fibers and pyramidal neurons with prominent, radially oriented apical dendrites are shown. This organization has the effect of restricting water displacement parallel to the cortical surface more than displacement orthogonal to it, resulting in diffusion ellipsoids which are non-spherical with their major axes oriented radially (arrows). By 35 weeks GA (*B*), prominent basal dendrites for the pyramidal cells and thalamocortical afferents have been added. This has the effect of restricting water displacement more uniformly in all directions. As a result, the diffusion ellipsoids are spherical, without a preferred orientation.

taking place in human cerebral cortex between 26 and 41 weeks GA correspond to the stage of 'cortical maturation' of Sidman and Rakic (Sidman and Rakic, 1982) or the 'perinatal period' of Marín-Padilla (Marin-Padilla, 1992). Early in this period, large pyramidal cells begin their maturation and extend dendrites into layer 1, along radial glial cells (Marin-Padilla, 1992). This organization may preferentially hinder water motion orthogonal to the cortical surface as compared with radial to it, accounting for both the relatively high anisotropy and the radial orientation of the major eigenvectors. Subsequently, this developmental period is characterized by progressive neuronal maturation. This includes formation of cell processes and their connections (Poliakov, 1959; Sidman and Rakic, 1982; Kostovic and Rakic, 1990), as well as the arrival of a large number of local circuit neurons and their differentiation in the cortical plate (Letinic and Rakic, 2002). These changes in microstructure may disrupt the initially more pronounced radial organization. By 36 weeks GA, the elaboration of basal dendrites of pyramidal cells, formation of local circuits, addition of thalamocortical afferent fibers (Kostovic and Rakic, 1990) and disappearance of radial glia (Sidman and Rakic, 1973, 1982) lead to roughly equivalent hindrance of water motion both orthogonal to the cortical surface and radial to it. This sequence of cellular events would explain the gradual loss of anisotropy which takes place between 26 and 36 weeks GA (Fig. 5). This pattern of anisotropy change is specific to cerebral cortex. Areas of high anisotropy in white matter areas generally show steadily increasing A_σ values with increasing GA (Huppi *et al.*, 1998; Neil *et al.*, 1998).

The reason for not consistently finding high anisotropy values in frontal cortex is not clear from this study. It is most likely due to the presence of bulk magnetic susceptibility effects in this area caused by the proximity of the air–tissue interface of the nasal cavity. These susceptibility effects disrupt the local static magnetic field, producing artifacts that interfere with the measurement of diffusion. Alternatively, it may represent a different pattern of maturation for frontal cortex. For example, it has been shown that formation of columns in the prefrontal cortex in primates precedes formation of columnar dominance columns in the visual cortex (Schwartz and Goldman-Rakic, 1991). Thus it is possible that, by 26 weeks GA, frontal cortex has already passed through the stage at which anisotropy values are high.

The finding that cortical D_{av} values increase between 26 and 32 weeks GA, then decrease from 32 to 41 weeks, is also unique to developing cortex. Previous studies have shown that D_{av} values decrease monotonically with increasing GA for all areas studied, including cerebral cortex (Huppi *et al.*, 1998; Neil *et al.*, 1998). However, neither of these studies included infants <30 weeks GA, so this phenomenon could not have been detected. Nevertheless, data from non-cortical brain areas – the head of the caudate (this study) and white matter areas (data not shown) – show a steady decrease of D_{av} values even before 30 weeks GA. For those brain areas which show a steady decrease in D_{av} values throughout development, this finding is readily explained by the dramatic decrease in water content which takes place during brain maturation (Dobbing and Sands, 1973). As water content decreases, barriers to motion move closer together, leading to a decrease in D_{av} values. For cortical plate, phenomena that could explain an increase rather than decrease in D_{av} values early during maturation include a decrease in cell density associated with programmed cell death (Bayer and Altman, 1991; Chan and Yew, 1998) and, in particular, the addition of neuropil between the neuronal somas (Bourgeois and Rakic, 1993). (This argument includes the assumption that neuropil has low hindrance to water motion as compared with cell somas, which is not proven.) Thus, it is plausible that competing mechanisms – addition of neuropil and programmed cell death versus decreasing water content – cause a rise in D_{av} values between 26 and 32 weeks GA, followed by a fall after 32 weeks GA.

In summary, this study represents the first characterization of the magnitude and orientation of water diffusion anisotropy in premature newborn human cerebral cortex. The dramatic changes in diffusion parameters which accompany cortical maturation parallel changes in the underlying cellular architecture. Diffusion methodology offers the potential for unique insight into the cortical development of both normal infants and those with brain injury. It may also be possible to detect alterations in cortical microstructure caused by various genetic and environmental factors (Rakic, 1988a; Volpe, 2001; Buxhoeveden and Casanova, 2002).

Notes

This research was supported by NIH grants NS37357 and CA83060. The authors thank Dr Brad Schlaggar for useful discussion and Dr Paul Thompson for assistance with statistical analysis.

Address correspondence to Jeffrey J. Neil, Pediatric Neurology, St Louis Children's Hospital, 1 Children's Place, St Louis, MO 63110, USA. Email: neil@wuchem.wustl.edu.

References

Ballard JL, Khoury JC, Wedig K, Wang L, Elerswalsman BL, Lipp R (1991) New Ballard score, expanded to include extremely premature infants. J Pediatr 119:417–423.

Baratti C, Barnett A, Pierpaoli C (1997) Comparative MRI study of brain maturation using T1, T2, and the diffusion tensor. In: Proceedings of the ISMRM, 5th Annual Meeting and Exhibition, p. 504. Vancouver: International Society for Magnetic Resonance in Medicine.

Basser PJ, Pajevic S, Pierpaoli C, Duda J, Aldroubi A (2000) *In vivo* fiber tractography using DT-MRI data. Magn Reson Med 44:625–632.

Bayer SA, Altman J (1991) Quantitative studies of the nuclear area and orientation in the developing neocortex. In: Neocortical development, pp. 106–115. New York: Raven Press.

Beaulieu C, Allen PS (1994) Determinants of anisotropic water diffusion in nerves. Magn Reson Med 31:394–400.

Bourgeois JP, Rakic P (1993) Changes of synaptic density in the primary visual cortex of the macaque monkey from fetal to adult stage. J Neurosci 13:2801–2820.

Brody BA, Kinney HC, Kloman AS, Gilles FH (1987) Sequence of central nervous system myelination in human infancy. I. An autopsy study of myelination. J Neuropathol Exp Neurol 46:283–301.

Buxhoeveden DP, Casanova MF (2002) The minicolumn hypothesis in neuroscience. Brain 125:935–951.

Chan WY, Yew DT (1998) Apoptosis and Bcl-2 oncoprotein expression in the human fetal central nervous system. Anat Rec 252:165–175.

Conturo TE, Lori NF, Cull TS, Akbudak E, Snyder AZ, Shimony JS, McKinstry RC, Burton H, Raichle ME (1999) Tracking neuronal fiber pathways in the living human brain. Proc Natl Acad Sci USA 96:10422–10427.

Cowan WM, Zipursky SL, Jessell TM (eds) (1997) Molecular and cellular approaches to neural development. New York: Oxford University Press.

Dobbing J, Sands J (1973) Quantitative growth and development of human brain. Arch Dis Child 48:757–767.

Honig LS, Herrmann K, Shatz CJ (1996) Developmental changes revealed by immunohistochemical markers in human cerebral cortex. Cereb Cortex 6:794–806.

Huppi PS, Maier SE, Peled S, Zientara GP, Barnes PD, Jolesz FA, Volpe JJ (1998) Microstructural development of human newborn cerebral white matter assessed *in vivo* by diffusion tensor magnetic resonance imaging. Pediatr Res 44:584–590.

Kostovic I, Rakic P (1990) Developmental history of the transient subplate zone in the visual and somatosensory cortex of the macaque monkey and human brain. J Comp Neurol 297:441–470.

Kostovic I, Judas M, Rados M, Hrabac P (2002) Laminar organization of

the human fetal cerebrum revealed by histochemical markers and magnetic resonance imaging. Cereb Cortex 12:536–544.
Letinic K, Rakic P (2001) Telencephalic origin of human thalamic GABAergic neurons. Nat Neurosci 4:931–936.
Letinic K, Rakic P (2002) Origin of GABAergic neurons in the human neocortex. Nature 417:645–646.
Marin-Padilla M (1992) Ontogenesis of the pyramidal cell of the mammalian neocortex and developmental cytoarchitectonics: a unifying theory. J Comp Neurol 321:223–240.
Mori S, Crain BJ, Chacko VP, van Zijl PCM (1999) Three-dimensional tracking of axonal projections in the brain by magnetic resonance imaging. Ann Neurol 45:265–269.
Mori S, Itoh R, Zhang J, Kaufmann WE, van Zijl PC, Solaiyappan M, Yarowsky P (2001) Diffusion tensor imaging of the developing mouse brain. Magn Reson Med 46:18–23.
Mountcastle VB (1997) The columnar organization of the neocortex. Brain 120:701–722.
Neil JJ (1997) Measurement of water motion (apparent diffusion) in biological systems. Concepts Magn Reson 9:385–401.
Neil JJ, Shiran SI, McKinstry RC, Schefft GL, Snyder AZ, Almli CR, Akbudak E, Aaronovitz JA, Miller JP, Lee BCP, Conturo TE (1998) Normal brain in human newborns: apparent diffusion coefficient and diffusion anisotropy measured using diffusion tensor imaging. Radiology 209:57–66.
Pierpaoli C, Jezzard P, Basser PJ, Barnett A, DiChiro G (1996) Diffusion tensor MR imaging of the human brain. Radiology 201:637–648.
Poliakov GI (1959) Progressive neuron differentiation of the human cerebral cortex in ontogenesis. In: Development of the central nervous system (Sarkisov SA, Preobrazenskaya SN, eds), pp. 11–26. Moscow: Medzig.
Rakic P (1972) Mode of cell migration to the superficial layers of fetal monkey neocortex. J Comp Neurol 145:61–84.
Rakic P (1988a) Defects of neuronal migration and pathogenesis of cortical malformations. Prog Brain Res 73:15–37.
Rakic P (1988b) Specification of cerebral cortical areas. Science 241:170–176.
Rubenstein JL, Rakic P (1999) Genetic control of cortical development. Cereb Cortex 9:521–523.
Schwartz ML, Goldman-Rakic PS (1991) Prenatal specification of callosal connections in rhesus monkey. J Comp Neurol 307:144–162.
Shimony JS, McKinstry RC, Akbudak E, Aronovitz JA, Snyder AZ, Lori NF, Cull TS, Conturo TE (1999) Quantitative diffusion-tensor anisotropy brain MR imaging: normative human data and anatomic analysis. Radiology 212:770–784.
Sidman RL, Rakic P (1973) Neuronal migration, with special reference to developing human brain: a review. Brain Res 62:1–35.
Sidman RL, Rakic P. (1982) Development of the human central nervous system. In: Histology and histopathology of the nervous system (Haymaker W, Adams RD, eds), pp. 3–145. Springfield, IL: C.C. Thomas.
Sorensen AG, Wu O, Copen WA, Davis TL, Gonzalez RG, Koroshetz WJ, Reese TG, Rosen BR, Wedeen VJ, Weisskoff RM (1999) Human acute cerebral ischemia: detection of changes in water diffusion anisotropy by using MR imaging. Radiology 212:785–792.
Thornton JS, Ordidge RJ, Penrice J, Cady EB, Amess PN, Punwani S, Clemence M, Wyatt JS (1997) Anisotropic water diffusion in white and gray matter of the neonatal piglet brain before and after transient hypoxia–ischaemia. Magn Reson Imaging 15:433–440.
Volpe JJ. (2001) Neurology of the newborn, 4th edn. Philadelphia, PA: W.B. Saunders.